Dynamic modelling of a submerged freeze microgripper using a thermal network.

Béatriz Lopez Walle, Michaël Gauthier, Nicolas Chaillet

Dynamic modelling of a submerged freeze microgripper using a thermal network

Beatriz López Walle, Michaël Gauthier, and Nicolas Chaillet

***Abstract*— Manipulating micro-objects whose typical size is under 100 μm becomes an interesting research topic for micro-assembly applications. A comparative analysis of dry and liquid media impacts on surface forces, contact forces and hydrodynamic forces showed that performing manipulation and assembly in liquid surroundings can indeed be more efficient than in dry conditions. We propose a thermal based micromanipulator designed to operate completely submerged in an aqueous medium. The handling principle and the advantages of our proposed submerged freeze microgripper against air working cryogenic grippers are first described. Then, the thermal principle based on Peltier effect, the characteristics of the prototype, and its first micromanipulation tests are reported. In order to manage the heat exchanges in the microgripper, a dynamic thermal model using electrical analogy has been developed for a 3D heat sink of the microgripper. Its validation is presented in the last section. Further works will be focused on the characterization of all the parameters and its experimental validation.**

I. INTRODUCTION

Extending manipulation process to the so-called microworld, i.e. typically between one micrometer and one millimeter, requires particularly efficient, reliable and precise handling strategies. During the last years, microgripping has received considerable research interest to perform these main tasks: picking up, moving and releasing the manipulated micro-object. Most of them are able to pick and move objects with acceptable performances; in contrast, releasing them with a good reliability and a high accuracy still remains a critical problem [1].

Release phase is strongly affected by surface forces, especially under 100 μm [2]. A comparative analyse in [3] clearly shows that: (i) surface forces (van der Waals force, electrostatic force) and contact force (pull-off force) reduce significantly in liquid medium; (ii) capillary force are completely cancelled in submerged conditions; (iii) hydrodynamic force increases in submerged environment. These phenomena reduce drastically the adhesion and electrostatic perturbations, and the loss of micro-objects thanks to the limitation of their maximal velocity. Performing manipulation tasks in submerged conditions represents thus a promising approach.

This work is supported by the Mexican National Council for Science and Technology (CONACYT), and the PRONOMIA project granted by the French National Research Agency (ANR)

Authors are with Lab. d'Automatique de Besançon, UMR CNRS 6596 - ENSMM - UFC, 24 rue Savary, 25000 Besançon, France `blopez@ens2m.fr`

This paper is focused on the study of a submerged freeze microgripper. Its handling strategy is shown in Fig. 1. Firstly, the gripper comes close to the object without touching it. Secondly, an ice droplet is generated holding just a small part of the object. The object can be then picked and positioned. Finally, the ice droplet thaws mixing with the water and the object is released without any influence of capillary force.

The thermal validation, which results are detailed in [4], has been modelled using the finite elements software (FEM) COMSOL Multiphysics 3.2.

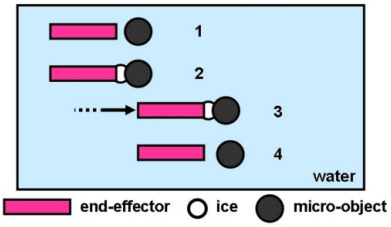

Fig. 1. Handling Strategy: (1) the micro-gripper approaches, (2) an ice droplet is generated and catches the object, (3) the object is manipulated, (4) the ice thaws and the object is liberated.

Ice grippers have been yet used for manipulating objects in air, as described in [5]–[8]. The dimensions of gripped objects are typically bigger than 200 μm and the main applications are optical, mechanical or electrical microcomponents assembly [6]. Cryogenic grippers provide high holding forces without introducing additional stress or damaging the surface of the manipulated micro-objects. Their handling abilities are almost independent of objects shape and material properties; even if low thermal conductive micro-objects seems recommended.

Their thermal principle is based either on Joule-Thompson effect, or Peltier effect. As they work in air ambient, water must be provided by an external device, and capillary force appears during the release because water does not evaporate completely. Then, they have to be combined with other release strategies to detach manipulated objects. In addition, they must work with particular environmental conditions like low temperature and low humidity. The miniaturization of these grippers is also limited by release difficulties.

The submerged freeze gripper proposed in this paper, profits from the advantages of submerged manipulation, particularly the cancellation of capillary force. Consequently, it can be extended to smaller

objects below 100 μm as typical size.

Analysing and understanding thermal phenomena appear very relevant to control and optimize the microgripper performances. One powerful method to simulate, and simplify, the complex heat exchanges involved in the submerged freeze microgripper is the use of thermo-electrical analogies. Nevertheless, classical electrical models correspond in general to planar thermal systems, and consequently, they can not be applied to our 3D device. An adapted thermal network would be developed. A static thermal model using electrical analogy for the Peltier elements and the 3D heat sinks of the microgripper has been described in [9]. In this paper, we propose a dynamical thermal modelling corresponding to our 3D device using thermal networks.

This paper is composed by the following sections. Section II describes the principle of the submerged freeze microgripper, the characteristics of the first prototype and the first results experimentations. Section III proposes a thermal network (a RC equivalent circuit) modelling the dynamic thermal problem of the 3D heat sinks. Finally, section IV shows the results of the comparison between the thermal network and a FEM simulation, that validates the proposed model.

II. THE EXPERIMENTAL DEVICE

We developed a first prototype of the submerged freeze gripper. Its principle based on Peltier effect, its physical and technical characteristics, and the first tests using it are presented in this section.

A. Submerged Freeze Gripper Principle

As described below, the submerged freeze gripper utilizes the water environment to create an ice droplet. The cooling energy for freezing water is provided by two Peltier thermoelectric components.

A Peltier module provides an electrical current-proportional generation or absorption of heat when direct current flows through it. The direction of the heat flow depends on the direction of the current, and the difference of temperatures caused by the heat transfer imposes two faces: a cold one and a hot one. The hot face must be associated to a heat sink in order to dissipate the heat flux.

As illustrated in Fig. 2, the submerged freeze system consists on two Peltier module stages, and a forced convection system. The first stage contains a Peltier micromodule named MicroPelt (μP). The end-effector is directly attached to its cold side. By this way, the MicroPelt can cool it and consequently generates the ice droplet on its acting part. The freezing process increases the temperature of the MicroPelt's hot face. Convection heat flow in water is thus so important than the whole system (liquid, gripper and Peltier micromodule) could warm up. To actively decrease the temperature at the MicroPelt's heat sink, a second Peltier element is connected. We called it MiniPeltier (mP). The temperature of its hot face must be constant to optimize its performance: it is maintained at the ambient temperature by forced convection using a liquid cooling system [9]. As MicroPelt's maximal cooling capacity is not sufficient to freeze the end-effector from ambient temperature, the liquid cooling system can not be used directly on its hot face.

The end-effector and the MicroPelt are completely submerged and electrically insulated. The MiniPeltier and the cooling liquid system stay in air to dissipate heat outside water.

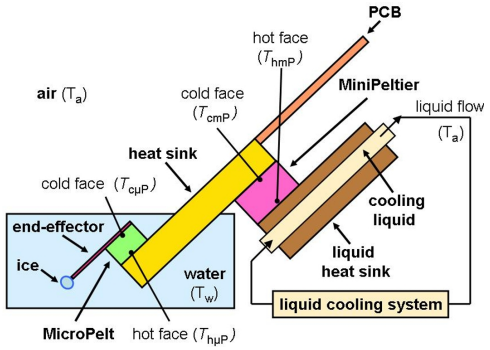

Fig. 2. Submerged Freeze System Principle.

B. Physical and Technical Characteristics

The first prototype of the submerged freeze gripper (without the end-effector) is shown in Fig. 3.

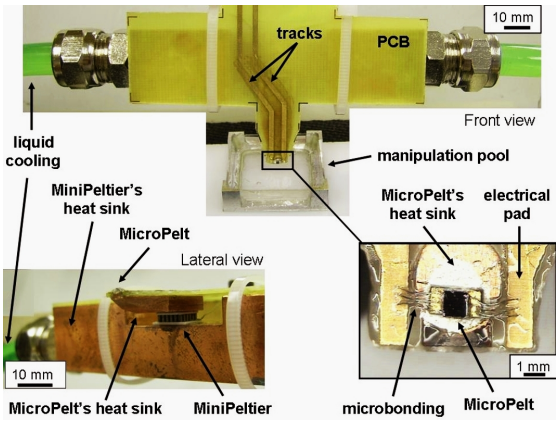

Fig. 3. Experimental freeze gripper.

The MicroPelt (Infineon Technologies AG) has as dimensions 720 $\times$ 720 $\times$ 428 μm^3. Its hot face is fastened to a copper heat sink (MicroPelt's heat sink). The MiniPeltier (Melcor FC0.6-18-05), which dimensions are 6.2 $\times$ 6.2 $\times$ 2.4 mm^3, is fixed on its cold face to the

MicroPelt's heat sink; and on its hot face to the copper liquid heat sink of the cooling liquid system.

A specific PCB has been fabricated to establish the electrical connections of both Peltier modules. Because of the very small dimensions of the MicroPelt, microbonding technology were used for its connections.

C. First Experimentations

The first experimentations using the prototype described above were performed in distilled water at 2 ^{o}C. The objectives were to validate the good working of the system and its reliability. For these first tests, the end-effector was not included.

Fig. 4 describes the tele-manipulation of a silicon object whose dimensions are: 600 × 600 × 100 μm^3. A pre-cooling phase is necessary to decrease the temperature of the MicroPelt's heat sink. During this phase, only the current in the MiniPeltier (i_{mP}) is applied and set constant at 0.9 A (Fig. 4a). When the temperature is about 0.5 ^{o}C (this temperature is sufficiently close to 0 ^{o}C but it prevents the heat sink to freeze), the MicroPelt is approached to the micro-object and its current ($i_{\mu P}$) is turned on at 0.5 A. The cooling energy generates the ice droplet (4 μl) which involves a part of the object in 3 s (Fig. 4b). The freeze gripper can thus displace it towards a new position (Fig. 4c). To release it, the MicroPelt's current is inverted at -0.3 A. The ice droplet thaws in 7 s and melts with the aqueous medium, liberating the micro-object without adhesion perturbations (Fig. 4d). The micromanipulation has been performed in 30 s. As previously mentioned, the cycle time for pick and release, obtained for optimal working conditions of the Peltier modules, is 3 + 7 = 10 s. The rest of the time, i.e. 20 s of transportation time in this case, depends principally on operator's ability, or microgripper speed in case of full automation. Contrary to the cryogenic grippers in air, capillary force does not perturb the release because the object and the MicroPelt are submerged. The Peltier currents choice is based on the thermal simulation presented in [4].

The same experiment was successfully repeated several times. The submerged freeze principle seems thus a promising approach to manipulate micro-objects. Further manipulations will be dedicated to objects sized under 100 μm.

The thermal management becomes a crucial part of the microsystem design. However, thermal processes of the submerged freeze gripper involves combined heat conduction and convection leading to a complex system. The definition of a control strategy requires a model of the thermal exchanges in the whole system. The next section deals with a thermal modelling by electrical analogy.

III. DYNAMIC THERMAL NETWORK

To predict and optimize the performances of the submerged freeze microgripper it is necessary to achieve a complete heat exchanges study. An equivalent electrical model, so-called thermal network, represents a relatively simple, but powerful tool for simulating the real system [10]. Used equivalences between thermal and electrical systems are summarized in table I. Furthermore, a thermal network notably allows to easily connect several thermal subsystems together. For these reasons, and considering the complexity of heat transfers on the submerged freeze gripper, we propose to build up its proper thermal network.

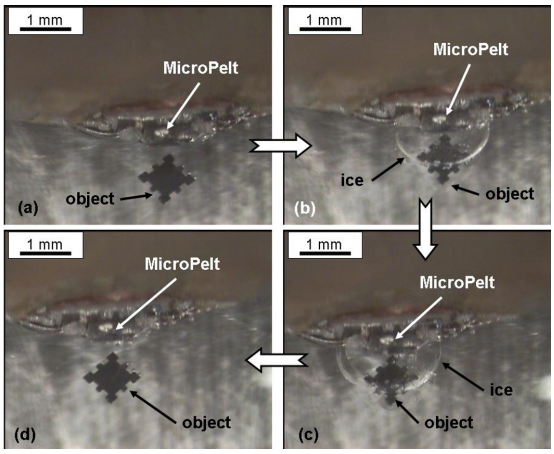

Fig. 4. Micromanipulation of a 600 × 600 × 100 μm^3 silicon object with the submerged freeze gripper.

TABLE I
THERMAL AND ELECTRICAL ANALOGY

Thermal system	**Equivalent electrical system**
Heat flux Q	Current i
Temperature difference ΔT	Voltage difference ΔV
Thermal resistance R_{th}	Resistance R

This section gives first the thermal network for a Peltier module; then we proposed a dynamical thermal network for a 3D heat sink.

A. Thermal Network for a Peltier Module

As described above, it is necessary to control the cold temperature of both Peltier elements, MicroPelt and MiniPeltier, via their electrical currents, to improve the performances of the submerged freeze microgripper.

In a Peltier module, cooling capacity Q_c and heating capacity Q_h are related to Peltier coefficient α, electrical resistance R, thermal conductivity coefficient k_P, electrical current supplied i, and temperature on cold and hot faces, T_c and T_h respectively. Their expressions can be written as:

$$Q_c = -\alpha T_c i + \frac{Ri^2}{2} + k_P(T_h - T_c) \quad (1)$$

$$Q_h = \alpha T_h i + \frac{Ri^2}{2} - k_P(T_h - T_c) \quad (2)$$

The steady-state thermal network for a Peltier module, based on (1) and (2), is described by [8]. Its equivalent electrical circuit is shown in Fig. 5. Peltier effect is represented by current source $P_S = \alpha T_c i$; Joule effect is modelled by current sources $P_{J/2} = Ri^2/2$; and the conductivity coefficient is analogous to the thermal resistance term, $R_{th} = 1/k_P$.

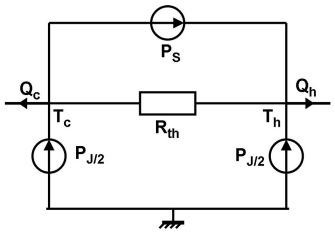

Fig. 5. Thermal network for a Peltier element [8].

A validation of this model applied to the MiniPeltier appears in [9].

B. Thermal Network for a 3D Element

To find the thermal network of the heat sinks and the end-effector, they are be considered as the block shown in Fig. 6. Heat flux $Q(x,t)$ through the block causes a gradient of temperature between the two lateral faces, and heat convection Q_h takes place from all other surfaces in contact with the external fluid whose temperature is T_{ext}.

Thermal networks are currently focused on planar systems, and the thermal network of the 3D case presented in Fig. 6 was not studied. We propose thus a thermal network model for this 3D system.

To determine the thermal network it is necessary to analyse the distribution of the temperature $T(x,t)$ in the block.

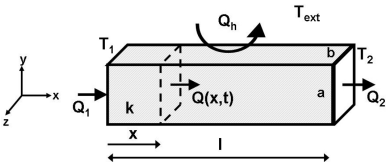

Fig. 6. Thermal schema for the heat sinks and the end-effector.

The length l is considered sufficiently bigger than the height a and the width b to neglect the variation of the temperature T along axes **y** and **z**. Consequently, the thermal problem is reduced to a one dimensional problem and the temperature in the block satisfies:

$$\alpha \frac{\partial^2 T}{\partial x^2} - \sigma(T - T_{ext}) = \frac{\partial T}{\partial t} \tag{3}$$

$$\text{where} \quad \alpha = \frac{k}{\rho C} \quad \text{and} \quad \sigma = \frac{\rho C S}{hP}. \tag{4}$$

The conduction heat transfer coefficient is k, the convection heat transfer coefficient is h, the density is ρ, the specific heat is C, the perimeter is $P = 2a + 2b$, and the section is $S = ab$.

The boundary conditions are defined by:

$$Q_1 = Q(0,t) = -kS \frac{\partial T}{\partial x}(0,t) \tag{5}$$

$$Q_2 = Q(l,t) = -kS \frac{\partial T}{\partial x}(l,t) \tag{6}$$

Applying the Laplace transform to $T(x,t)$, such as $\theta = \theta(x,p) = Laplace[T(x,t)]$ with $T(x,0) = T_{ext}$, (3) can be written as:

$$\frac{1}{q^2}\frac{d^2\theta}{dx^2} - \theta = -\theta_{ext} \tag{7}$$

$$\text{where} \quad q^2 = \frac{p+\sigma}{\alpha} \quad \text{and} \quad \theta_{ext} = \frac{T_{ext}}{p}. \tag{8}$$

In the same way, the Laplace transform is applied to the boundary conditions (5) and (6):

$$\phi_1 = Laplace\,[Q_1] = -kS \frac{d\theta}{dx}(0,p) \tag{9}$$

$$\phi_2 = Laplace\,[Q_2] = -kS \frac{d\theta}{dx}(l,p) \tag{10}$$

The solution of (7) considering (9) and (10) is thus:

$$\theta(x,p) = \frac{\phi_1 ch(ql) - \phi_2}{kSq \cdot sh(ql)} ch(qx) - \frac{\phi_1}{kSq} sh(qx) + \theta_{ext} \tag{11}$$

Heat flux ϕ_1 and ϕ_2 can be thus deduced as a function of $\theta_1 = \theta(0,p)$ and $\theta_2 = \theta(l,p)$:

$$\phi_1 = -\frac{\theta_{ext} - \theta_1}{z_2} + \frac{\theta_1 - \theta_2}{z_1}, \tag{12}$$

$$\text{and } \phi_2 = -\frac{\theta_2 - \theta_{ext}}{z_2} + \frac{\theta_1 - \theta_2}{z_1}, \tag{13}$$

where the impedances z_1 and z_2 are:

$$z_1 = \frac{sh(ql)}{kSq} \tag{14}$$

$$z_2 = \frac{sh(ql)}{kSq(ch(ql) - 1)} \tag{15}$$

To find the linear thermal impedances z_{1lin} and z_{2lin}, the infinite series expansion when $(ql) \to 0$ is done to (14) and (15):

$$z_{1lin} = R_{c0} \tag{16}$$

$$z_{2lin} = \frac{1}{\frac{1}{R_{v0}} + pC_{th0}} \tag{17}$$

where the conduction thermal resistance R_{c0}, the convection thermal resistance R_{v0} and the thermal capacitor C_{th0} are respectively:

$$R_{c0} = \frac{l}{kS} \tag{18}$$

$$R_{v0} = \frac{2}{hPl} \tag{19}$$

$$C_{th0} = \frac{\rho C S l}{2} \tag{20}$$

Inserting (16), (17) in (12), (13), ϕ_1 and ϕ_2 are now:

$$\phi_1 = -\frac{\theta_{ext} - \theta_1}{R_{v0}} - pC_{th0}(\theta_{ext} - \theta_1) + \frac{\theta_1 - \theta_2}{R_{c0}} \tag{21}$$

$$\phi_2 = -\frac{\theta_2 - \theta_{ext}}{R_{v0}} - pC_{th0}(\theta_2 - \theta_{ext}) + \frac{\theta_1 - \theta_2}{R_{c0}} \tag{22}$$

Applying the inverse Laplace transform, they become:

$$Q_1 = -\frac{T_{ext} - T_1}{R_{v0}} + C_{th0}\frac{dT_1}{dt} + \frac{T_1 - T_2}{R_{c0}} \tag{23}$$

$$Q_2 = -\frac{T_2 - T_{ext}}{R_{v0}} - C_{th0}\frac{dT_2}{dt} + \frac{T_1 - T_2}{R_{c0}} \tag{24}$$

The thermal network for the block described in Fig. 6 is thus represented by Fig. 7.

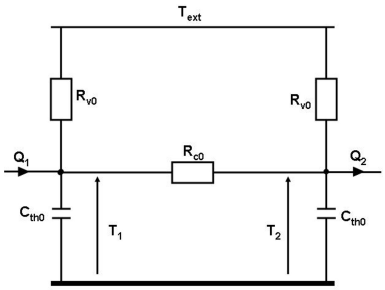

Fig. 7. Thermal network for the heat sinks and the end-effector.

This thermal network has a validity condition because it has been obtained thanks to the linearisation of z_1 and z_2. So, it is only valid when z_1 and z_2 are near to z_{1lin} and z_{2lin}, respectively. Impedances (14) and (15) can be also written as:

$$z_1 \approx \frac{l}{kS}\left(1 + \frac{(ql)^2}{6}\right) = z_{1lin}\left(1 + \frac{(ql)^2}{6}\right) \tag{25}$$

$$z_2 \approx \frac{2}{kSlq^2}\left(1 + \frac{(ql)^2}{12}\right) = z_{2lin}\left(1 + \frac{(ql)^2}{12}\right) \tag{26}$$

The thermal network model is valid if at least:

$$\left|\frac{(ql)^2}{6}\right| \ll 1 \tag{27}$$

In case of $p = j\omega$, and remembering (8), condition (27) is expressed by:

$$\omega^2 \ll \omega_v^2 \tag{28}$$

where $\omega_v^2 = \frac{36\alpha^2}{l^4} - \sigma^2$.

For a steady-state modelling ($w = 0$), the condition of validity, introducing (4), is thus defined by:

$$l^2 < \frac{6kS}{hP} \tag{29}$$

Considering (28), for a dynamic modelling the poles p_1 and p_2 of the thermal network have to respect:

$$|p_1| \ll \omega_v^2, \tag{30}$$

$$\text{and } |p_2| \ll \omega_v^2. \tag{31}$$

From (23) and (24), the poles can be calculated as:

$$p_1 = -\frac{1}{R_{v0}C_{th0}} \tag{32}$$

$$p_2 = -\frac{R_{c0} + 2R_{v0}}{R_{c0}R_{v0}C_{th0}} \tag{33}$$

Decomposing the terms, conditions (30) and (31) become respectively:

$$l^2 \ll \frac{6kS}{\sqrt{2}hP} \tag{34}$$

$$l^2 \ll \frac{\left(\sqrt{14} - 2\right)kS}{hP} \tag{35}$$

Comparing (34) and (35), the thermal network dynamic model is valid if:

$$\nu \ll 1 \tag{36}$$

where $\nu = \frac{l^2}{\frac{(\sqrt{14}-2)kS}{hP}}$.

In the next section, we compared the thermal network to FEM simulations.

IV. VALIDATION OF THE DYNAMIC THERMAL NETWORK

To validate the thermal network, the temperatures $T_1(t) = T(0,t)$ and $T_2(t) = T(l,t)$ have been calculated in air and water using FEM calculations simulated with COMSOL Multiphysics 3.2, and comparing them to the equivalent electrical model in Fig. 7. Different geometries has been compared in both media. Two examples are presented in this paper, where the heat flux applied are such as $Q_1(t \geq 0) = Q(0, t \geq 0) = 0.66$ W and $Q_2(t \geq 0) = Q(l, t \geq 0) = 2.98$ W; zero elsewhere.

Table II shows the criterion ν for both geometries analysed in water. The first case corresponds to the MicroPelt's heat sink.

Fig. 8 presents the curves obtained with geometry I, while Fig. 9 illustrates the curves obtained with geometry II.

In Fig. 9, the thermal networks curves are closer to the FEM curves than in Fig. 8. In fact, the criterion ν of the

TABLE II
GEOMETRIES AND THEIR VALIDATION PARAMETER IN WATER

Case	Geometry (mm)	Criterion ν (36)
I	$a = 2$, $b = 7$, $l = 11$	0.35
II	$a = 2$, $b = 7$, $l = 3$	0.03

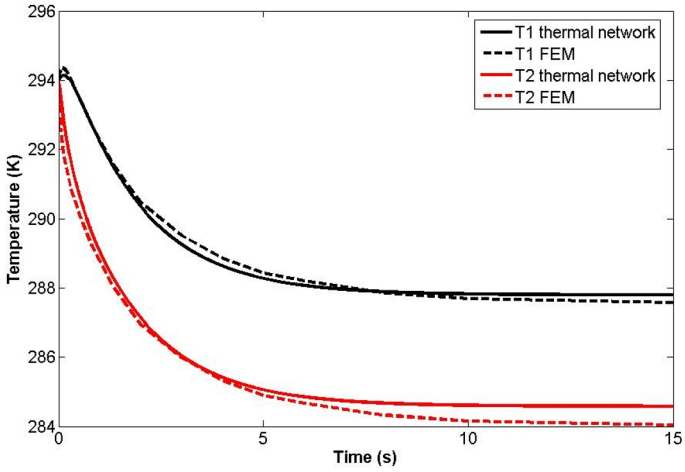

Fig. 8. T_1 et T_2 for the geometry I in water

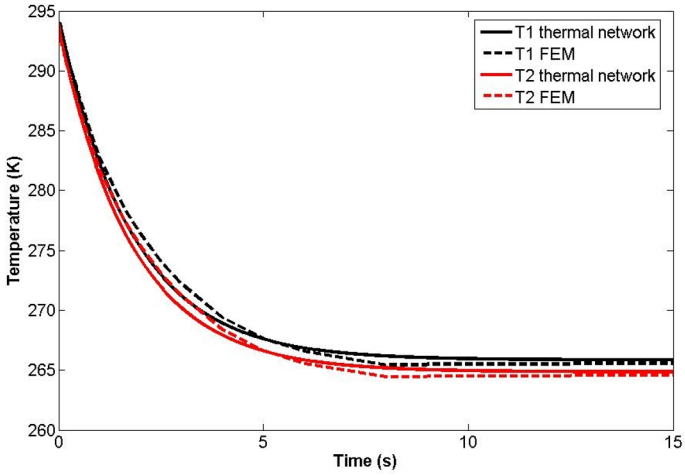

Fig. 9. T_1 et T_2 for the geometry II in water

second geometry is better than the criterion ν of the first one.

Furthermore, the results obtained during the comparison between the FEM calculation and the thermal network let us validated this one. In particular, resulting curves for the geometry I, which represents a direct application of our system, are very pertinents for our proposes.

The characterization of the parameters involved in the whole thermal network and its experimental validation is under development. A whole system thermal network will then estimate properly heat processes and optimize the submerged freeze microgripper.

V. CONCLUSIONS

One of the principal challenges to execute efficient micromanipulations stays in performing handling strategies. These ones are permanently influenced by surfaces forces above all during the release phase. A comparative study of the dealings of dry and liquid media on surface forces, contact forces, and hydrodynamic forces shown the advantages of the submerged micromanipulations. This new approach fosters us to develop an innovative micromanipulation strategy adapted to the aquatic medium. The submerged freeze microgripper presented in this paper exploits the liquid medium to generate an ice droplet at the active part of the end-effector to pick up the micro-object. To release it, the ice is thawed without having any influence of the capillary force.

Being the optimization and control of the heat exchanges a crucial part to perform the submerged freeze microgripper, an equivalent dynamical electrical model is proposed: a new dynamical thermal network for a 3D heat sink has been developed and compared to a FEM model. The equivalent electrical model seems sufficiently accurate for our application case.

Further works will be focused on the characterization of the parameters involved in the whole thermal network and its experimental validation. In the next step, this model will allow us to control the temperature and thickness of the ice microdrop in order to manipulate micro-objects under the 100 μm.

VI. ACKNOWLEDGEMENTS

The authors would like to thank Micropelt GmbH for providing the MicroPelt Peltier coolers.

REFERENCES

[1] D. S. Haliyo and S. Régnier. Advanced applications using micromad, the adhesion based dynamic micro-manipulator. In *In Proc. of AIM*, pages 880–885, Port Island, Japan, July 2003.
[2] M. Gauthier, B. López-Walle, and C. Clévy. Comparison between micro-objects manipulations in dry and liquid mediums. In *Proc. of the 6th CIRA*, Espoo, Finland, June 2005.
[3] M. Gauthier et al. Forces analyses for micromanipulations in dry and liquid media. *Journal of Micromechatronics*, 3(3-4):389–413, September 2006.
[4] B. López-Walle, M. Gauthier, and N. Chaillet. Submerged freeze gripper to manipulate micro-objects. In *Proc. IEEE/RSJ IROS*, Beijing, China, October 2006.
[5] D. Lang, M. Tichem, and S. Blom. The investigation of intermediates for phase changing micro-gripping. In *Proc. of the Int. Workshop on Microfactories*, Besancon, France, October 2006.
[6] J. Liu, Y.-X. Zhou, and T.-H. Yu. Freeze tweezer to manipulate mini/micro objects. *JMM*, 14(2):269–276, February 2004.
[7] S. Droz et al. New generation of grippers for the manipulation of miniaturized components. In *Proc. of Mechatronics*, pages 572–575, Besançon, France, October 2001.
[8] G. Seliger, J. Stephan, and S. Lange. Hydroadhesive gripping by using peltier effect. In *Proc. of IMECE*, pages 3–8, Florida, USA, November 2000.
[9] B. López-Walle, M. Gauthier, and N. Chaillet. A submerged freeze microgripper for micromanipulations. In *Proc. IEEE ICRA*, Roma, Italy, April 2007.
[10] J. P. Holman. *Heat transfer*. Mac Graw Hill, 1990.